

# A prediction methodology for the high cycle fatigue life of hydrogen-loaded structures

Wissam Bouajila\*, Jörg Riccius\*, Matthias Bruchhausen\*\*, Burkhard Fischer\*\*

\**Deutsches Zentrum für Luft- und Raumfahrt (DLR) – Lampoldshausen, Institute of Space Propulsion  
Im Langen Grund, D-74239 Hardthausen, Germany*

\*\**European Commission, Joint Research Centre, Institute for Energy and Transport  
P.O. Box 2, 1755 ZG Petten, The Netherlands*

## Abstract

An ultrasonic high cycle fatigue (HCF) test bench was used for a detailed experimental investigation of the quantitative influence of internal hydrogen on the HCF life of Inconel X-750<sup>®</sup> in the hydrogen concentration range from 5 to 39 wppm at ambient temperature. For an alternating stress equal to 0.6 times the yield stress of the hydrogen-free material and zero mean stress, a drop of two orders of magnitude in the high-cycle fatigue durability of the material has been measured over the investigated hydrogen concentration range. New Finite Element (F.E.) analysis post processing tools have been developed to predict with relatively little effort the drop in life duration due to internal hydrogen embrittlement at steady state hydrogen concentration conditions. The core of this proposed F.E. calculation-based method is the “Wöhler surface”, i.e. a conventional Wöhler curve extended by the hydrogen concentration as the third dimension. A two-step validation / verification of this F.E. post processing analysis method has been performed.

## 1. Introduction

Hydrogen embrittlement is not completely understood despite intense investigation [1]. It should be recognized that there is no single mechanism causing hydrogen embrittlement. Apparently different mechanisms apply to different systems under various conditions. Recently, several mechanisms have been proposed by different researchers as: hydrogen pressurization [2] [3] [4], hydrogen-induced decohesion [5] [6] and hydrogen enhanced localized plasticity (HELP) [1] [7] [8] [9].

The aim of this investigation is to study the influence of internal hydrogen on the HCF life duration of Inconel X-750<sup>®</sup> and to propose a methodology that considers the hydrogen embrittlement of the material to accurately predict the high-cycle durability of a structure considering the deleterious effects of hydrogen with little effort. In the framework of the In Space Propulsion project (ISP1), an original ultrasonic HCF test bench has been designed to provide experimental data for the analyses. The numerical simulations of the reduction in life due to internal hydrogen embrittlement were performed using a commercial F.E. program e.g. Ansys<sup>®</sup>.

## 2. Material and experimental procedure

### 2.1. Investigated material

A metal or alloy prone to hydrogen embrittlement is required in order to get a clear picture of the influence of hydrogen on the material behavior and to well assess the validity of the hydrogen embrittlement modeling with high accuracy.

Therefore, the nickel-based superalloy Inconel X-750<sup>®</sup> has been selected for this study in order to assess the accuracy of the numerical simulation of hydrogen embrittlement of metals and alloys. Inconel X-750<sup>®</sup> is commonly used in aerospace applications (gas turbine blades, seals, combustors and others components) and is reported to show a significant susceptibility to hydrogen embrittlement. Moreover, detailed data concerning physical properties and hydrogen embrittlement-related parameters of Inconel X-750<sup>®</sup> are available in open literature.

The batch of Inconel X-750<sup>®</sup> investigated in this study was ordered with the specification AMS 5667 M and heat treated to HTH conditions i.e. solution annealed at 1366.5 K (2000 °F) for 1 hour, rapidly cooled and aged at 977.6 K (1300 °F) for 20 hours to get a material structure similar to the structure of the material whose parameters regarding the hydrogen embrittlement model are available in open literature. The composition of the tested Inconel X-750<sup>®</sup> is given in Table 1.

Table 1 : Chemical analysis of the used Inconel X-750<sup>®</sup> (in % weight)

Ni	Cr	Fe	Ti	Nb	Al	other
71.6	15.5	8.2	2.5	1.0	0.7	0.5

## 2.2. Procedure and conditions of the charging of the material with hydrogen

HCF test samples from Inconel X-750<sup>®</sup> were singly charged with gaseous hydrogen prior to testing. The charging of the samples with hydrogen was performed at a temperature of 873 K with pressurized gaseous hydrogen. Each sample was clamped at one end, free on the other end, and heated by induction at its central part.

In this work, the duration for a complete charging of the material with hydrogen is defined as the minimal time to reach equilibrium between the hydrogen concentration on the sample surface and the hydrogen concentration in the sample center. At the end of the charging process, the hydrogen is assumed to be uniformly distributed in the sample. Equilibrium can be assumed as being reached either for a rate of hydrogen in the material  $\chi = 80\%$  according to Anyalebechi et al. [10] or for a hydrogen concentration ratio  $\omega(r=0) = 99.9\%$  according to Deng et al. [11]. In this work, equilibrium has been assumed to be reached for  $\omega(r=0) = 99.95\%$ . A charging duration of 80 minutes has then been used for each test sample to be fully charged with gaseous hydrogen.

The pressure of gaseous hydrogen applied during the charging stage is determined by the charging temperature and the aimed hydrogen concentration through Sievert's law. The gaseous hydrogen pressures applied during the sample charging process are listed in Table 2.

Table 2 : Applied hydrogen pressure for the charging of the HCF test samples made from Inconel X-750<sup>®</sup> according to the aimed hydrogen concentration in the material.

Aimed hydrogen concentration (in wppm)	GH2 pressure @ 873K (in bar)
5	1
18	12.5
39	60

## 2.3. High cycle fatigue testing of the hydrogen-charged samples

### 2.3.1. Presentation of the HCF test setup

Fatigue tests in the HCF and very high cycle fatigue (VHCF) regime, i.e. beyond  $10^6$  cycles are often carried out by means of ultrasonic excitation at 20 kHz since this technique allows reaching a high number of cycles in a very short time [12]. In this section, firstly the concept of ultrasonic fatigue testing is introduced; then the actually used testing device is shortly presented. A more detailed description of the setup can be found in [13].

In an ultrasonic HCF test rig, a piezoelectric converter is used to generate mechanical oscillations in axial direction of the test sample at a frequency of about 20 kHz. These oscillations are amplified by means of an acoustic horn and finally applied to the specimen. The components of the load train (acoustic horn and specimen) are dimensioned so that a standing wave can form. The lengths of the horn and the specimen are chosen so that a node of displacement (which coincides with a maximum of axial stress) is located at the center of the specimen. Once the system has been calibrated, the stress amplitude  $\sigma_{am}$  can be controlled by the AC voltage driving the piezoelectric converter.

A schematic of the HCF test bench developed in the framework of the ISP1 project is shown in Figure 1. The specimen is attached to the top horn via the threaded tip. The pressure chamber can be filled with gaseous hydrogen up to 350 bar.

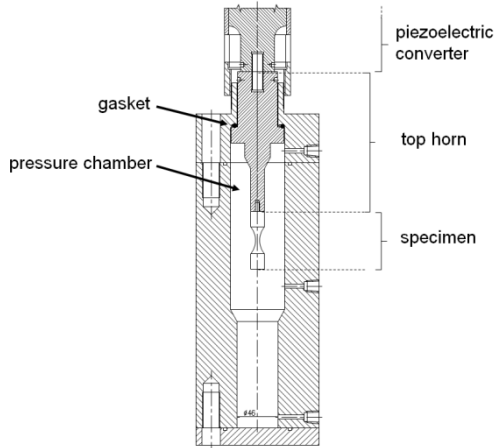


Figure 1 : Schematic of the used ultrasonic HCF test bench (autoclave and load train).

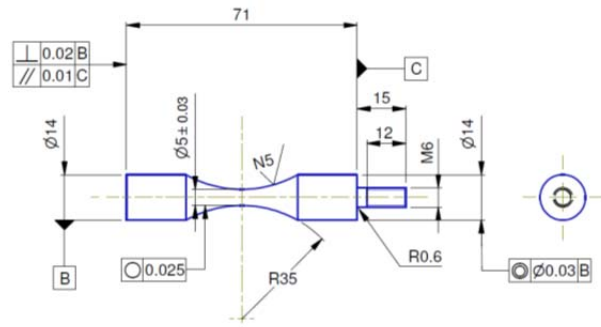


Figure 2 : Geometry of the ultrasonic HCF test sample made from Inconel X-750® (dimensions in mm).

### 2.3.2. HCF tests conditions

The dependency of life duration of Inconel X-750® on both, the applied alternating stress level and the hydrogen concentration was investigated. The HCF tests have been performed at a frequency of 20 kHz and at room temperature in a pressurized autoclave in symmetric push-pull mode (stress ratio  $R_\sigma = -1$ ). The hydrogen-charged samples were tested in pressurized gaseous hydrogen to prevent outgassing of dissolved hydrogen from the material. The value of the hydrogen pressure is set so that the gaseous hydrogen is in equilibrium with the hydrogen in the material. An alternating stress value and a hydrogen concentration are defined for each HCF test. All the HCF tests were repeated once to enhance the reliability of the experimental data. The dependency of the number of cycles to failure on the alternating stress level has been investigated only for a single hydrogen concentration (18 wppm) and the dependency of the number of cycles to failure on the hydrogen concentration has been investigated only for a single alternating stress ( $0.6\sigma_0^{RT}$  where  $\sigma_0^{RT}$  is the yield stress of the hydrogen-free material at room temperature) as illustrated with the dashed blue lines in Figure 3. Three values for the alternative stress ( $0.5\sigma_0^{RT}$ ,  $0.6\sigma_0^{RT}$ , and  $0.7\sigma_0^{RT}$ ) and three hydrogen concentrations (5, 18, and 39 wppm) have been considered for the HCF test campaign.

### 2.3.3. HCF test sample geometry

The HCF tests were carried out on hourglass-shaped specimens. The sample dimensions are calculated considering the stress that will be applied during the test and the mechanical properties of the constitutive material [13]. The geometry and the dimensions of the HCF test sample made from Inconel X-750® are given in Figure 2.

### 2.3.4. HCF tests results

The HCF tests results are summarized in Figure 3 where the number of cycles to failure of the HCF test samples made from Inconel X-750® is plotted as a function of the applied alternating stress and the hydrogen concentration in the material.

Despite the scatter in the experimental data, the number of cycles to failure for Inconel X-750® shows a strong sensitivity to both, the applied stress amplitude and the hydrogen concentration in the material. As observed by Balitskii et al. for Ni-alloys [14], the material shows a decrease of its HCF life with increasing alternating stress for a constant hydrogen concentration. The increase of the hydrogen concentration in the material results in a strong reduction of the HCF life duration of the alloy for a constant alternating stress. Globally, the HCF life duration of Inconel X-750® has been reduced by two orders of magnitude over the observed ranges of alternating stress and hydrogen concentration. This result underlines the strong HCF life reducing effect of hydrogen on the numbers of cycles to failure of Inconel X-750®.

In addition to determining the magnitude of the deleterious effect of hydrogen on the HCF life of the investigated material, the experimental data will be used as input for a Finite Element simulation of the HCF life reduction of Inconel X-750® samples due to internal hydrogen.

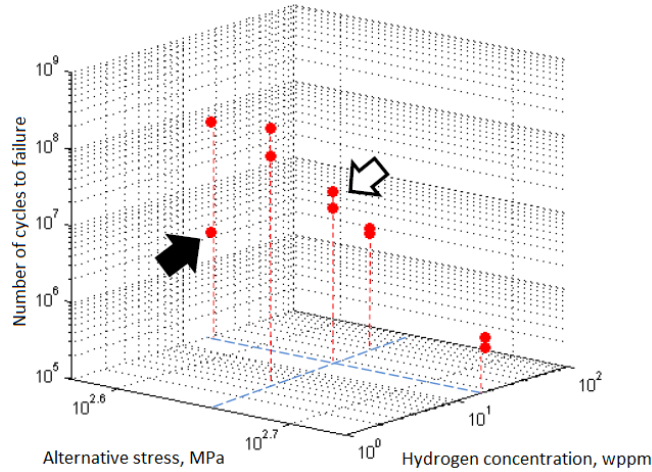


Figure 3 : Ultrasonic HCF tests results for Inconel X-750<sup>®</sup> – Evolution of the number of cycles to failure as a function of the applied alternative stress ( $R_{\sigma} = -1$ ) and the hydrogen concentration in the material at 293 K.

### 3. Calculation of the hydrogen concentration

#### 3.1. Hydrogen concentration at steady-state condition

Dissolved hydrogen in metals and alloys is assumed to reside either at normal interstitial lattice sites (NILS) or reversible trapping sites at micro-structural defects generated by plastic deformation. The two populations are assumed to always be in equilibrium according to Oriani's theory [15]. The assumption of local equilibrium can be used when the trap filling kinetics are very rapid as it is usually the case [16]. Assuming that both, lattice and trap sites constitute finite populations and furthermore assuming no interaction between occupied sites, one may write

$$\frac{\theta_T}{1 - \theta_T} = \frac{\theta_L}{1 - \theta_L} K_T \quad (1)$$

where  $\theta_L$  denotes the occupancy of the NILS,  $\theta_T$  denotes the occupancy of the trapping sites,

$$K_T = \exp\left(-\frac{W_B}{RT}\right) \quad (2)$$

represents the equilibrium constant,  $W_B$  is the (inherently negative) trapping binding energy,  $R$  is the gas constant equal to  $8.31 \text{ J}\cdot\text{mol}^{-1}\cdot\text{K}^{-1}$  and  $T$  is the absolute temperature.

The hydrogen concentration at trapping sites,  $C_T$ , in hydrogen atoms per unit volume, can be expressed as

$$C_T = \theta_T \alpha N_T \quad (3)$$

where  $\alpha$  denotes the number of sites per trap and  $N_T$  denotes the trap density measured in number of traps per unit lattice volume. Two different models for calculating the trap density,  $N_T$ , are available depending on the nature of the trapping sites. The first model assumes that hydrogen is trapped at the interface between the metal matrix and the second phase precipitates, thus sets a constant value for the trap density. The second model considers that hydrogen trap sites are associated only with dislocations in the deforming metal. Assuming one trap site per atomic plane threaded by a dislocation [17] [18] [19], the trap site density in traps per cubic meter is given by [20]

$$N_T = \sqrt{2} \rho / a \quad (4)$$

where  $a$  is the lattice parameter and  $\rho = \rho(\varepsilon^p)$  denotes the dislocation density as a function of the local plastic straining measured in terms of the effective plastic strain  $\varepsilon^p$ .

The hydrogen concentration in the NILS,  $C_L$ , in hydrogen atoms per unit volume, can be stated as

$$C_L = \theta_L \beta N_L \quad (5)$$

where  $\beta$  denotes the number of NILS per atom solvent, and  $N_L$  denotes the number of solvent lattice atoms per unit lattice volume. If the available number of trapping sites per unit volume,  $\alpha N_T$ , is small compared to the available NILS per unit volume,  $\beta N_L$ , then

$$N_L = N_A/V_M \quad (6)$$

in which  $N_A = 6.0232 \times 10^{23}$  atoms per mole is the Avogadro's number and  $V_M$  is the molar volume of the host lattice measured in units of volume per lattice mole.

For a mechanically stressed material, hydrogen concentrations in the NILS are studied under equilibrium conditions with the local stress  $\sigma_{ij}$ . The Fermi-Dirac form [21] is used to calculate, for a system under external stress, the equilibrium hydrogen concentration  $C_L$  in terms of the initial (in the absence of stress) hydrogen concentration in the NILS,  $C_L^0$ :

$$\frac{\theta_L}{1 - \theta_L} = \frac{\theta_L^0}{1 - \theta_L^0} K_L \quad (7)$$

where  $\theta_L^0 = C_L^0/(\beta N_L)$  denotes the initial (in the absence of stress) NILS occupancy,

$$K_L = \exp\left(\frac{\sigma_h V_H}{RT}\right) \quad (8)$$

is the equilibrium constant dominated by the first-order interaction of hydrogen with stress,  $\sigma_h = \sigma_{kk}/3$  is the local hydrostatic stress, and  $V_H$  is the partial molar volume of hydrogen in solution. The assumption of a purely dilatational distortion is known to be correct for a first order approximation [22]. Except for very high pressures, Sievert's law can be used for gaseous hydrogen environments, to relate the external hydrogen pressure,  $P_{H_2}$  to the concentration of hydrogen in a stress-free region of the metal lattice

$$C_L^0 = k \sqrt{P_{H_2}} \quad (9)$$

where  $k = k_0 \exp(-\Delta H_0/(RT))$  is the Sievert's constant.

Denoting  $c_L$  as the hydrogen concentration in the NILS measured in units of hydrogen atoms per solvent atom

$$c_L = C_L/N_L = \beta \theta_L \quad (10)$$

with  $\theta_L = \theta_L^0 K_L / (1 + \theta_L^0 (K_L - 1))$  using Eq. (7). The relationship between the corresponding measures for the initial NILS concentration in the stress-free lattice is  $c_L^0 = C_L^0/N_L$ .

Similarly, a hydrogen concentration at trapping sites  $c_T$  measured in trapped hydrogen atoms per solvent atom is introduced

$$c_T = C_T/N_L = \beta \theta_{TL} \quad (11)$$

Combining Eq. (1) and Eq. (3) yields to

$$\theta_{TL} = \frac{\alpha N_T}{\beta N_L} \frac{\theta_L K_T}{(1 + \theta_L (K_T - 1))} \quad (12)$$

Combining Eq. (10) and Eq. (11) finally results in defining the total hydrogen concentration  $c$ , measured in hydrogen atoms per solvent atom, as

$$c = c_L + c_T = \beta (\theta_L + \theta_{TL}) \quad (13)$$

Equation (13) defines the total hydrogen concentration at a material spot as a function of the effective plastic strain  $\varepsilon^p$ , the hydrostatic stress  $\sigma_h$ , and the initial hydrogen concentration  $C_L^0$  in the stress-free lattice. In this formulation no transient effects [23] are accounted for in the hydrogen population development.

For HTH Inconel X-750<sup>®</sup>, the initial hydrogen concentration in the NILS measured in wppm was defined by the following version of Sievert's law [24]  $c_L^0 = 39.25 \sqrt{P_{H_2}} \exp(-6850/(RT))$  where  $P_{H_2}$  is the hydrogen pressure in MPa,  $R$  is the universal gas constant (8.314 J/mol K) and  $T$  is the absolute temperature in K. The trap binding energy,  $W_B$ , is assumed to be equal to -15.1 kJ/mol [25]. The trap site density,  $N_T$ , is defined as a constant value of  $6.0 \times 10^{26}$  trap sites per cubic meter [25] based on the assumption that hydrogen is trapped at the octahedral sites on the interface between the matrix and the  $\gamma'$  precipitates in the Inconel X-750<sup>®</sup> lattice. The parameter  $\alpha$  is assumed to be equal to 1. The parameter  $\beta$  is set equal to 1 with octahedral site occupancy.

### 3.2. Validation of the prediction of the hydrogen concentrations

The assessment of the reliability of the parameters available in open literature for HTH Inconel X-750 and their suitability for the material investigated in this study as well as the validity and accuracy of the equations used for the calculation of the hydrogen concentration was performed by comparing the predictions of the set of equations to experimental hydrogen concentration measurements for various hydrogen pressures and temperatures.

#### 3.2.1. Hydrogen charging conditions and measurement accuracy

Tensile test samples made from Inconel X-750<sup>®</sup>, whose shape and dimensions are shown in Figure 4, have been used for the charging of the material with hydrogen. The samples were charged with pressurized gaseous hydrogen at a temperature of about 973 K. To do so, each sample was installed in a tensile test machine equipped with a pressurized autoclave. As shown in Figure 5, the sample was clamped at its upper end, free at its bottom end, and heated by induction at its center. The whole sample was covered with ceramic wool in order to reduce heat loss by free convection and radiation at high temperature.

In this analysis, the dependency of the hydrogen concentration in the material on the pressure of the gaseous hydrogen was investigated considering two values of the hydrogen pressure: 10 and 30 bar.

Although the sample was covered using ceramic wool, a temperature gradient along the sample was observed due to heat conduction through the top clamping system. This variation of temperature along the sample was used to assess the dependency of the hydrogen concentration in the material on temperature. Nine bores were drilled along the sample to install the thermocouples for measuring the temperature along the axis of the sample. As illustrated in Figure 4, seven thermocouples were installed over the parallel length area with one at the center of the sample (position 0) and the others installed on either side of the center and at every 3 mm. The last two thermocouples are located at 19.5 mm either side of the sample center.

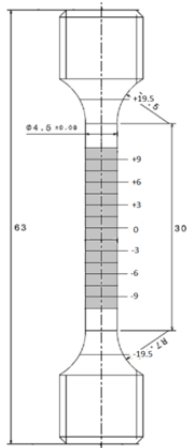


Figure 4 : Shape and dimensions of the tensile test samples made from Inconel X-750<sup>®</sup> and locations of the 9 thermocouples.



Figure 5 : Picture of the equipment used for the heating of the tensile test sample: the sample is clamped at its top and covered with ceramic wool.

The temperature distribution along the axis of the sample (i.e. at the center of the sample, position 0, and at every 3 mm away from the center) for an applied gaseous hydrogen pressure of 30 bar is plotted in Figure 6. As expected, the different thermal boundaries conditions at the ends of the sample have resulted in a non-uniform and non-symmetric temperature distribution along the specimen. A repetition of the test highlights a temperature scattering. Various possible reasons for this scatter of the measured temperature data have been identified:

- Positioning and fixation differences of the ceramic wool used to thermally insulate the specimen
- Scatter of the temperature measurement itself (including thermocouple positioning differences as well as scatter of components such as AD converters, amplifiers, ...)

A total scatter of 2.5% was observed at the center of the sample, which can be interpreted as a temperature measurement accuracy. Therefore, a constant uncertainty of 2.5% is assumed for the value of the measured temperature in the following discussion.

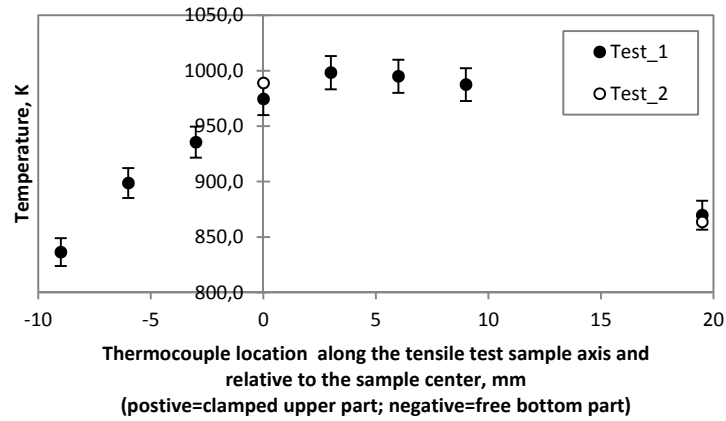


Figure 6 : Temperature profile along the axis of the tensile test sample made from Inconel X-750<sup>®</sup> under an applied gaseous hydrogen pressure of 30 bar. The sample was covered with ceramic wool and the heating power was set to deliver a temperature at the sample center of about 973K. The test has been performed twice.

### 3.2.2. Uncertainty in the calculated hydrogen concentration value

In this section of the paper, the propagation of the uncertainties of the experimental measurements of both the hydrogen pressure and temperature along the sample axis to the uncertainty of the calculated hydrogen concentration values is investigated.

From Eq. (13), and for a stress-free material, the uncertainty in the total hydrogen concentration  $c^0$ ,  $\Delta c^0$ , is defined as

$$\Delta c^0 = |\Delta c_L^0| + |\Delta c_T^0| \quad (14)$$

where  $\Delta c_L^0$  and  $\Delta c_T^0$  are the uncertainties of the hydrogen concentration in the lattice  $c_L^0$  and in the traps  $c_T^0$  for a stress-free material, respectively.

As  $c_L^0$  and  $c_T^0$  are dependent on the hydrogen pressure  $P_{H_2}$  and temperature  $T$  (cf. Eq. (9) through Eq. (12)), the uncertainty in  $c_L^0$ ,  $\Delta c_L^0$ , and the uncertainty in  $c_T^0$ ,  $\Delta c_T^0$ , with respect to the measurement accuracy of  $P_{H_2}$  and of  $T$ , can be approximated using partial derivatives:

$$\Delta c_L^0 = \left| \frac{\partial c_L^0}{\partial P_{H_2}} \right| \Delta P_{H_2} + \left| \frac{\partial c_L^0}{\partial T} \right| \Delta T \quad (15)$$

$$\Delta c_T^0 = \left| \frac{\partial c_T^0}{\partial P_{H_2}} \right| \Delta P_{H_2} + \left| \frac{\partial c_T^0}{\partial T} \right| \Delta T \quad (16)$$

With an accuracy of 0.25% for the pressure transducer used for measuring the hydrogen pressure and with considering the already discussed uncertainty of 2.5% in the measurement of the temperature, the uncertainty in the calculated hydrogen concentration in the material at steady-state conditions is about 1.5% for the considered gaseous hydrogen pressures and over the measured temperature range.

### 3.2.3. Measurement of the hydrogen concentration

Tensile test samples made from Inconel X-750 have been charged with hydrogen at a temperature of about 973 K in pressurized gaseous hydrogen without applying mechanical loading. The sample is assumed to be fully charged with hydrogen after a charging duration of 80 minutes. The applied hydrogen pressure is proportional to the square of the aimed hydrogen concentration in the material.

The hydrogen analysis has been performed by instrumental gas analysis (IGA). The hydrogen contained in the material is released using a vacuum heating degassing technique. Since the amount of material used for the analysis is limited to about 500 mg per measurement, the parallel length area of each hydrogen-charged tensile test sample was cut in seven cylindrical probes of 2.2 mm height centered at the temperature measurement spots as illustrated in Figure 4.

The accuracy of the measurement by IGA of the hydrogen concentration in the material is about 5 %.

### 3.2.4. Assessment of the reliability of the calculated hydrogen concentration

The calculated hydrogen concentrations are compared to the measurements obtained by IGA for hydrogen charging pressures of 10 and 30 bar in Figure 7 and Figure 8, respectively. Considering the measurement accuracy of 5 % and the uncertainty in the calculated hydrogen concentration of 1.5%, the predicted hydrogen concentrations show a quite good agreement with the measurements for the two charging conditions. The qualitative dependency of the hydrogen concentration on pressure is well simulated since the calculated hydrogen concentration increases when the pressure increases as observed with the measurement. The qualitative dependency of the experimentally determined hydrogen concentration on temperature is correctly obtained by the model as well since the calculated distribution of hydrogen is not uniform and proportional to the temperature value as underlined by the measurements.

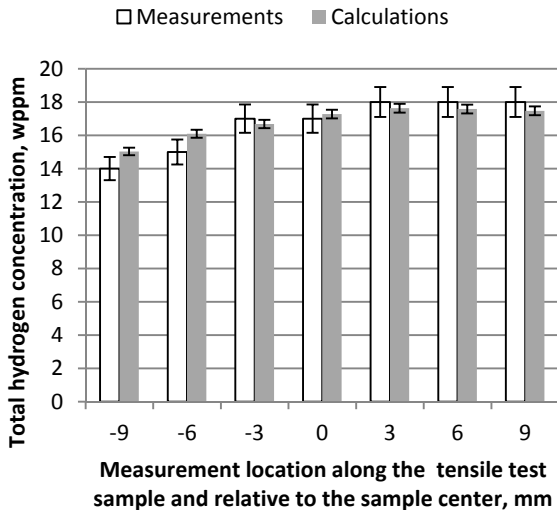


Figure 7 : Comparison of the calculated and the measured hydrogen concentration for several sections over the parallel length of the tensile test sample made from Inconel X-750 charged with gaseous hydrogen at about 973 K at a pressure of 10 bar.

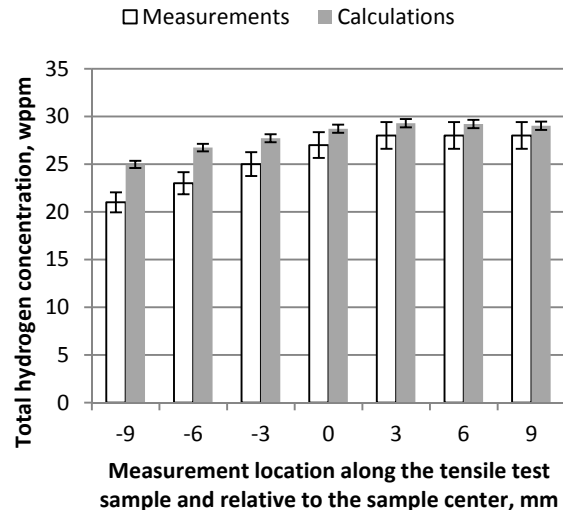


Figure 8 : Comparison of the calculated and the measured hydrogen concentration for several sections over the parallel length of the tensile test sample made from Inconel X-750 charged with gaseous hydrogen at about 973 K at a pressure of 30 bar.

Based on the results of the comparative analyses, the set of equations used for the calculation of the hydrogen concentration can be assumed reliable in the prediction of the hydrogen concentration in a material. The values of the coefficients for HTH Inconel X-750, available in open literature, could be considered accurate enough to be used for the material investigated in the present work.

## 4. Prediction of the HCF life duration considering internal hydrogen embrittlement

A simple approach has been developed within the framework of the ISP1 project to calculate as a first assessment the HCF life duration of a structure considering internal hydrogen embrittlement for a steady state hydrogen concentration condition. Hereby, the number of cycles to failure of the structure is defined as dependent on both the stress state of the structure and the hydrogen concentration. In a first step, the accuracy of the suggested simulation approach is assessed by comparing the predicted life duration of a HCF test sample to its corresponding measured number of cycles to failure for a defined loading case.

### 4.1. Suggested methodology

An original and intuitive analysis method has been developed in order to take into account the effect of hydrogen on the HCF life of a structure under external mechanical cyclic loads. This Finite Element calculation-based method can provide designers with a first approximation of the number of cycles to failure of a structure considering the external loading and the deleterious effect of internal hydrogen on the fatigue strength of the material. The flowchart in Figure 9 schematically illustrates the three main steps of the calculation methodology. The core of this Finite

Element calculation-based method is the “Wöhler surface”, i.e. an extended Wöhler curve with hydrogen concentration as the third dimension.

In a first step, the operating conditions of the structure are taken into account for the calculation of the stress state and the hydrogen distribution in the structure by performing a thermo-structural Finite Element analysis. Once this first step is completed, the resulting couple of stress and hydrogen concentration ( $\sigma, c$ ) is retrieved at every node  $i$  of the modeled structure and the corresponding number of cycle to failure  $N_{f,i}(\sigma, c)$  is determined based on the defined “Wöhler surface”. The HCF life duration of the structure  $N_f$  will correspond to the lowest calculated value of the number of cycles to failure  $N_{f,i}(\sigma, c)$ . For the currently presented work, the last two steps are performed using the post processor of Ansys®.

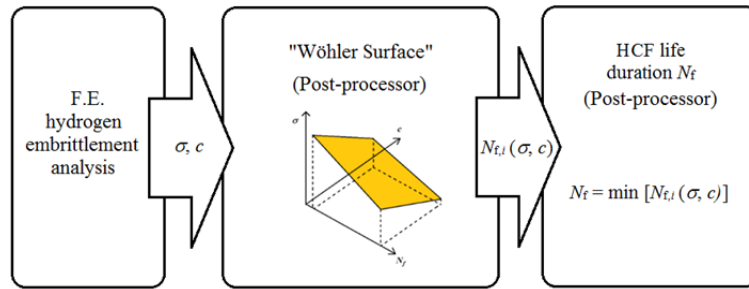


Figure 9 : Flowchart of the “Wöhler surface” methodology used to determine the high cycle fatigue (HCF) life duration of a structure considering internal hydrogen embrittlement.

#### 4.2. Implementation of the hydrogen embrittlement model into a Finite Element program

As an attractive alternative to a time-consuming in-house development of complex hydrogen embrittlement modeling codes, an intuitive methodology for the implementation of hydrogen embrittlement models into commercial F.E. programs has been suggested in the framework of the ISP1 project [26] [27]. This implementation methodology consists in a script that uses the usual commands and tools from a commercial F.E. program (Ansys® in this work). For the case of an isothermal temperature distribution, a reduced version of the implementation methodology is presented in [26].

Depending on the sensitivity of the mechanical properties of the material on hydrogen, one of the two versions of the implementation process has to be favored: the coupled-iterative approach (CIA) or the direct approach (DA). The consistency of these two approaches has been assessed by the comparison of the results from the F.E. simulation of an ultrasonic HCF test sample loaded in non-isothermal conditions with and without considering the influence of hydrogen in [27].

As demonstrated in [27], if the material shows no dependency of its elastic properties on hydrogen and as long as the hydrogen induced strain is negligible compared to the total strain and the elastic domain is not exceeded during the loading, the dependency of the stress and the strain on the hydrogen concentration can be neglected. In this case, the simple direct approach (DA) can be used instead of the more complicated and time-consuming coupled-iterative approach (CIA) to implement the hydrogen embrittlement model into a F.E. program.

As the elastic properties of Inconel X-750® are not too sensitive to hydrogen [28], the direct approach (DA) is used in this work to implement the hydrogen embrittlement model into the commercial F.E. program Ansys®.

#### 4.3. Definition of the “Wöhler surface” for Inconel X-750®

The “Wöhler surface” for Inconel X-750® is defined using the measurements from the HCF test campaign. Some of the results of the HCF tests summarized in Figure 3 will be used to define a “Wöhler surface” for Inconel X-750®.

##### 4.3.1. Considered HCF tests results

As illustrated in Figure 3, a test performed at  $\sigma_a = 0.5\sigma_0^{RT}$  and  $c_H = 18$  wppm (black arrow) shows an exceptional low number of cycles to failure. This low life duration could e.g. be the result of some macroscopic internal material defects. Therefore, this value of the life duration is excluded from the data base as used for the definition of the “Wöhler surface”.

A Finite Element simulation of the test conditions ( $\sigma_a = 0.6\sigma_0^{RT}$ ,  $c_H = 18$  wppm) will be later used for a first assessment of the accuracy of the Wöhler surface-based approach for comparing the predicted fatigue life to the

corresponding measurements. Consequently, the test data at this condition (white arrow in Figure 3) are also not used for the determination of the “Wöhler surface”.

As a result of the restrictions listed previously, only the data provided by the HCF tests performed at the range limits of either the alternative stress ( $0.5\sigma_0^{RT}$  and  $0.7\sigma_0^{RT}$ ) or the hydrogen concentration (5 wppm and 39 wppm) are used for the determination of the “Wöhler surface” (red dots in Figure 10).

#### 4.3.2. Defined “Wöhler surface” for Inconel X-750<sup>®</sup>

The plot shown in Figure 3 highlights that the obtained data of the tests performed at an alternating stress of  $0.6\sigma_0^{RT}$  and of those performed at a hydrogen concentration of 18 wppm could be fitted with straight lines in the log-log scale, respectively. Accordingly, the experimental life duration could be fitted with a plane in the 3-D log-log-log scale. The result of the fit of the selected experimental number of cycles to failure for Inconel X-750<sup>®</sup> using Matlab<sup>®</sup> is shown in Figure 10. The fit, which shows a good agreement with the experimental data, defines the “Wöhler surface” for Inconel X-750<sup>®</sup> at 293 K and will be used for the simulations in the following section.

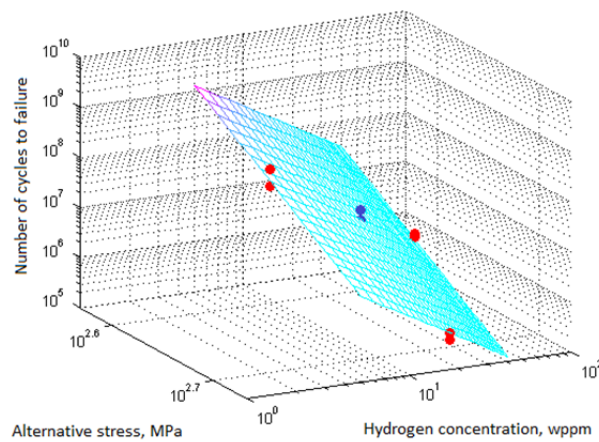


Figure 10 : “Wöhler surface” for Inconel X-750<sup>®</sup> at 293 K as determined from experimental measurements (only the red dots were used for the fit, the blue dots are used to assess the accuracy of the F.E. simulations).

#### 4.4. Simulation of the reduction in HCF life duration due to hydrogen embrittlement

The shortening effects of internal hydrogen on the fatigue life duration of an Inconel X-750<sup>®</sup> ultrasonic HCF test sample cyclically loaded in a gaseous hydrogen atmosphere as shown in Figure 3 will be simulated using the commercial Finite Element program Ansys<sup>®</sup> and the suggested Wöhler surface-based approach. As the elastic properties of Inconel X-750<sup>®</sup> are not too sensitive to hydrogen, the direct approach (DA) is used to implement the hydrogen embrittlement model into the program. The obtained values of  $(\sigma, c)$  will be considered as input values for the Wöhler surface-based method (see Figure 9). Since the samples are firstly charged with hydrogen at elevated temperature and then tested at ambient temperature, the Finite Element analysis will be performed in two separate steps. The HCF test (blue dots in Figure 10) with the following conditions will be simulated to assess the accuracy of the Finite Element simulation results:

- Step 1: Charging with hydrogen under the following (stress free) conditions:
  - Charging temperature: 873 K
  - Charging pressure: 12.5 bar
- Step 2: HCF testing under the following conditions:
  - Testing temperature: 293 K
  - Testing pressure: 40 bar
  - Alternative stress:  $0.6\sigma_0^{RT}$
  - Mean stress: 0 MPa

The resulting maximal hydrogen concentration for both, pre-charging and testing is 18 wppm.

As a first assessment of the accuracy of the simulation, the calculated number of cycles to failure for the HCF test sample geometry will be compared to the experimental data.

#### 4.4.1. Finite Element analysis of hydrogen embrittlement with Ansys®

- *Geometry and model mesh*

In order to compare the simulation results to experimental data, the geometry of the ultrasonic HCF test sample made from Inconel X-750® as shown in Figure 11 has been chosen for the Finite Element analysis. The dimensions of this sample are summarized in Figure 2. Since the test specimen is axisymmetric and shows a plane of symmetry at its center, only one quarter of it has been modeled for the calculations. The modeled and meshed geometry is superposed to the sample picture in Figure 11.

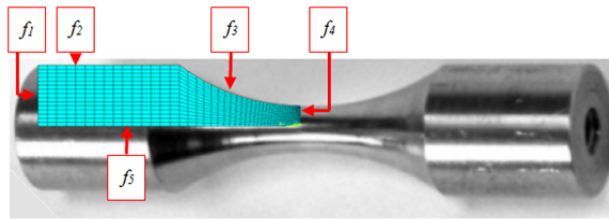


Figure 11 : Ultrasonic HCF test sample with the geometry modeled for the F.E. analysis, and the numbering of the five defined faces.

- *Mechanical properties*

Based on tensile tests results, the Young's modulus for Inconel X-750® is considered to be not influenced by hydrogen. It is assumed to steadily decrease with increasing temperature [29]. The Poisson's ratio for Inconel X-750® is assumed as 0.29 [20]. The values of the model's parameters for Inconel X-750® - as needed for the hydrogen embrittlement modeling - are given in section 3.1.

- *Finite Element simulation of the charging with hydrogen (Step 1)*

The numerical simulation was set up to model the hydrogen distribution resulting from charging the sample with hydrogen. The charging of the sample with gaseous hydrogen was performed at high temperature. The sample is clamped at one end and heated in its center using an induction coil. This results in a temperature gradient along the sample. As one sample end is free, no stress is induced by the thermal staining during the heating.

Although the boundary conditions are different for both sample ends, the temperature distribution along the sample is assumed symmetrical relative to the sample center in this paper. Therefore, the heating procedure is approximated in the thermal analysis by applying a heat flux through the face  $f_3$  of the model and defining convection on the face  $f_2$  and conduction on the face  $f_1$  (see Figure 11).

The value of the heat flux and the parameters for the convection and conduction have been set in order to reach a maximal temperature of 873 K at the center part of the sample (face  $f_4$ ) and to get a temperature difference of 150 K between the center part of the sample (face  $f_4$ ) and its clamping ends (face  $f_1$ ).

The evolutions of temperature and hydrogen concentration in axial direction of the sample along the axis of symmetry (face  $f_5$ ) are compared in Figure 12. These results show that the dependency of the hydrogen concentration on temperature is well reproduced by the modeling since the evolution of the hydrogen concentration is proportional to the evolution of temperature. Based on the simulation, the maximal hydrogen concentration of 18 wppm is reached on the outer surface, at the center of the sample (face  $f_4$ ), where the temperature is maximal.

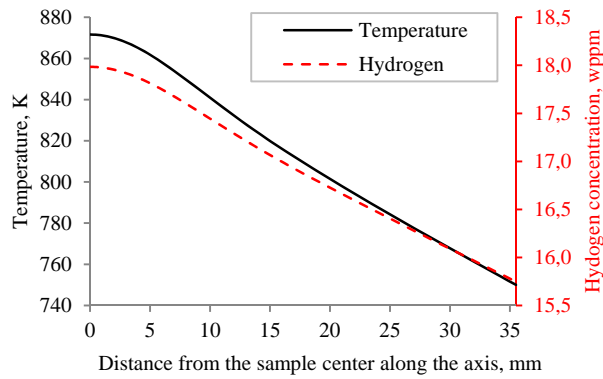


Figure 12 : Evolutions of temperature and hydrogen concentration along the axis of symmetry of the sample obtained for the F.E. simulation of the charging of a HCF test sample made from HTH Inconel X-750<sup>®</sup> with gaseous hydrogen at about 873 K and 12.5 bar.

#### 4.4.2. Finite Element simulation of the HCF test with hydrogen

During the HCF tests, the mechanical loading of the sample is obtained by exciting the sample to its eigenfrequency of the longitudinal (axial) mode by periodically applying a small displacement at the top end of the sample. The amplitude of the exciting signal is proportional to the targeted stress value in the middle (half-length) of the sample [13]. For the hydrogen-charged samples, the tests are performed under pressurized gaseous hydrogen to prevent outgassing of hydrogen from the material during testing.

Regarding the Finite Element simulations, several assumptions are made for simplification purposes. The test specimen is assumed to be loaded at both ends, so displacement control is applied on the face  $f_1$  of the model while symmetry conditions are assumed for faces  $f_4$  and  $f_5$  (see Figure 11).

As the HCF tests are performed for a stress ratio of  $R_\sigma = -1$ , the induced mean stress is equal to zero. An alternative stress of  $\sigma_a = 0.6\sigma_0^{RT}$  is considered for the analysis as previously explained. Due to the experimental cyclic loading path characteristics and for simplification purposes, the equivalent static load case with  $\sigma = \sigma_a$ , as indicated by the dashed red line in Figure 13, could be considered as a relevant alternative load for the structural analysis according to [30]. In the Finite Element simulation, the axial displacement value is set so that the resulting maximal axial stress is equal to  $0.6\sigma_0^{RT}$  at 293 K.

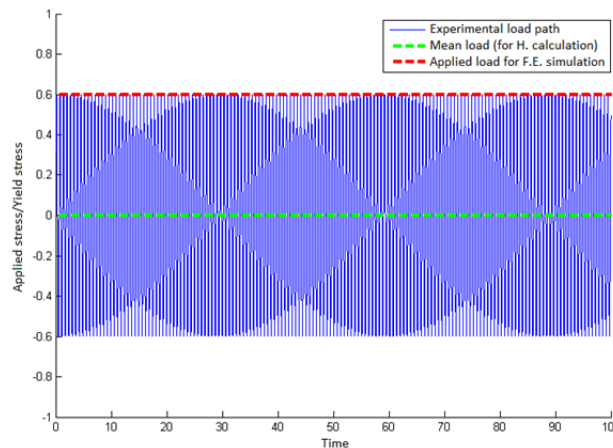


Figure 13 : Simplification of the assumed mechanical load to a constant value (red line) for the Finite Element analysis due to the nature of the very high frequency cyclic experimental load path. For non-zero mean stress conditions, the mean load (green line) would be taken into account to update the hydrogen concentration according to the resulting stress field.

In general, the hydrogen distribution depends on the stress state in the specimen. For the performed HCF tests, the frequency of the alternating stress is too high to have an impact on the hydrogen distribution so the mean stress should be used to take into account the redistribution of hydrogen in the specimen due to the applied mechanical load. In this case however, the mean stress is zero throughout the specimen as illustrated with the dashed green line in Figure 13, so the actual distribution of hydrogen can be considered to be independent from the stress state.

The prediction of the life duration of the hourglass-shape HCF test sample tested at  $\sigma_a = 0.6\sigma_0^{RT}$  and for  $c_H = 18$  wppm by F.E. simulation and using the defined “Wöhler surface” (see Figure 10) is shown in Figure 14. This figure shows the distribution of the number of cycles to failure calculated at each node of the model taking into account the simulation conditions for which the hydrogen concentration evolution is shown in Figure 12. In addition to the prediction of the life duration of the sample, this plot allows to predict the localization of a potential fracture area. The hydrogen-charged specimen shows the lowest number of cycles to failure at the area where both the stress and the hydrogen concentration are at their maximal values.

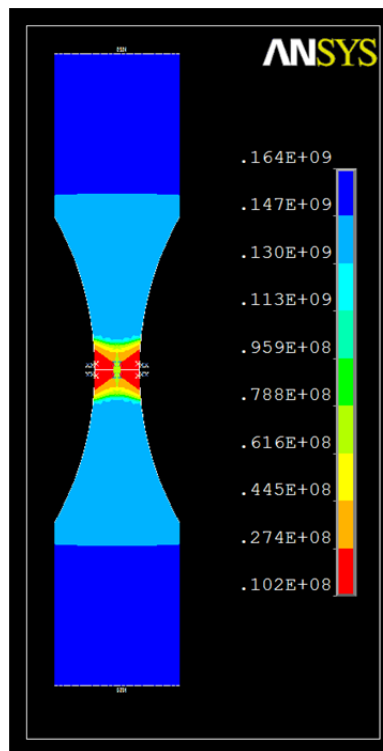


Figure 14 : Results of the simulation of the HCF test of a sample pre-charged with hydrogen with a maximal hydrogen concentration of 18 wppm and tested at ambient temperature at an alternative stress equal to 0.6 times the yield stress of the hydrogen-free material and a zero mean stress: life duration of the sample and localization of the failure area (red color area).

#### 4.4.3. Verification of the Finite Element simulation of the HCF test with hydrogen

The predicted life duration of the HCF test sample made from Inconel X-750<sup>®</sup> is compared to the measured number of cycles to failure as given in Table 3. The simulated number of cycles to failure of the HCF test sample shows a good agreement with the experimental measurements. Indeed, the predicted life duration is close to the life duration obtained for Test 1 and is within the scattering of the experimental results. These good results underline the promising capability of the proposed methodology to provide an accurate first assessment of the reduction in life duration of a structure due to hydrogen embrittlement with relatively little effort.

Table 3 : Comparison of the number of cycles to failure of a HCF test sample made from Inconel X-750<sup>®</sup> predicted by F.E. simulation to the experimental measurements at 293K and for a hydrogen concentration of 18 wppm. The sample is loaded at an alternating stress equal to 0.6 times the yield stress of the hydrogen-free material and zero mean stress.

Result of	Life duration (in cycles)
Test 1	1.00e7
Test 2	1.60e7
F.E. simulation	1.02e7

## 5. Conclusion

The ultrasonic HCF tests performed at a frequency of 20 kHz with hydrogen-precharged samples made from Inconel X-750<sup>®</sup> in pressurized gaseous hydrogen have highlighted a strong deleterious effect of internal hydrogen on the HCF life duration of this material with a drop of two orders of magnitude of the high-cycle fatigue durability over the investigated hydrogen concentration range from 5 to 39 wppm at ambient temperature.

By also considering the range of alternating stresses  $0.5\sigma_0^{RT}$  -  $0.7\sigma_0^{RT}$  where  $\sigma_0^{RT}$  is the yield stress of the hydrogen-free material at ambient temperature, the HCF test results have been used to define a "Wöhler surface" for Inconel X-750<sup>®</sup>. This extended Wöhler curve with hydrogen concentration as the third dimension is the core of an original Finite Element calculation-based method that has been developed to provide a first estimate of the number of cycles to failure of a structure considering the external loading and the deleterious effect of internal hydrogen on the fatigue strength of the material, and to locate the most probable fracture area in the structure.

Regarding the calculation of the hydrogen concentration in the material, the reliability of the parameters available in open literature for HTH Inconel X-750<sup>®</sup> and their suitability for the material investigated in this study have been validated with experimental measurements of the hydrogen concentration by IGA.

Despite of the considered assumptions for simplification purposes, the Finite Element analysis of an ultrasonic high-cycle fatigue test with a hydrogen-charged hourglass-shape sample from Inconel X-750<sup>®</sup> using the Wöhler surface-based approach has shown an accurate prediction of the reduction in HCF durability of the structure as the calculated HCF fatigue life of the sample was within the scattering of the corresponding measured number of cycles to failure. This simulation result is a first evidence of the strong capability of the developed Wöhler surface-based methodology to accurately predict the deleterious effects of internal hydrogen on the high-cycle fatigue durability of structures.

## 6. Acknowledgement

The research leading to the results described in this paper has received funding from the European Union Seventh Framework Programme under the grant agreement n° 218849.

## 7. References

- [1] H. Birnbaum and P. Sofronis, "Hydrogen enhanced localized plasticity - a mechanism for hydrogen related fracture," *Master. Sci & Eng.*, vol. A 176, pp. 191-202, 1994.
- [2] C. Zapffe and C. Sims, "Hydrogen embrittlement, internal stress and defects in steels," *Transactions of Metallurgical Society AIME*, vol. 145, pp. 225-261, 1941.
- [3] A. Tetelman and W. Robertson, "The mechanism of hydrogen embrittlement observed in iron-silicon crystals," *Transactions of the Metallurgical Society AIME*, vol. 224, pp. 775-783, 1962.
- [4] Y. Tong and J. Knott, "Evidence of the discontinuity of hydrogen-assisted fracture in mild steel," *Scripta Metallurgica*, vol. 25, pp. 1651-1656, 1991.
- [5] A. Troiano, "The role of hydrogen and other interstitials in the mechanical behavior of metals," *Transactions of ASM*, vol. 52, pp. 54-80, 1960.
- [6] H. Johnson, J. Morlet and A. Troiano, "Hydrogen, crack initiation, and delayed failure in steel," *Transactions of the Metallurgical Society AIME*, vol. 212, pp. 528-536, 1958.
- [7] C. Beachem, "A new model for hydrogen-assisted cracking (hydrogen "embrittlement")," *Metallurgical Transaction*, vol. 3, pp. 427-451, 1972.
- [8] C. Beachem, "Electron fractographic support for a new model for hydrogen assisted cracking," *Stress Corrosion Cracking and Hydrogen Embrittlement of Iron Base Alloys*, no. 5, pp. 376-381, 1977.

- [9] P. Sofronis and H. Birnbaum, "Mechanics of the hydrogen-dislocation-impurity interactions: part I-increasing shear modulus," *Journal of the Mechanics and Physics of Solids*, vol. 43, pp. 49-90, 1995.
- [10] P. Anyalebechi, D. Talbot and D. Granger, "The solubility of hydrogen in solid binary Aluminum-Lithium alloys," *Metallurgical Transactions B*, vol. 20B, pp. 523-533, 1989.
- [11] B. Deng, Q. Huang, L. Peng, O. Mao, J. Du, Z. Lu and X. Liu, "Measurement of hydrogen solubility, diffusivity and permeability in HR-1 stainless steel," *Journal of nuclear materials*, pp. 653-656, 1992.
- [12] H. Mayer, „Fatigue crack growth and threshold measurements at very high frequencies,“ *International Material Review*, Bd. I, Nr. 44, pp. 1-34, 1999.
- [13] M. Bruchhausen, P. Hähner, B. Fischer and D. Cornu, "Device for carrying out environmental High Cycle Fatigue tests with ultrasonic excitation in asymmetric push-pull mode," *International Journal of Fatigue*, vol. 52, pp. 11-19, 2013.
- [14] A. Balitskii, V. Vytvytskyi, L. Ivaskevich und J. Elias, „The high- and low-cycle fatigue behavior of Ni-contain steels and Ni-alloys in high pressure hydrogen,“ *International Journal of Fatigue*, Nr. 39, pp. 32-37, 2012.
- [15] R. Oriani, "The diffusion and trapping of hydrogen in metals," *Acta. Met.*, vol. 18, pp. 147-157, 1970.
- [16] P. Sofronis and R. McMeeking, "Numerical analysis of hydrogen transport near a blunting crack tip," *J. Mech. Phys. Solids.*, vol. 37, no. 3, pp. 317-350, 1989.
- [17] G. Thomas, "Hydrogen trapping in FCC metals," *Hydrogen Effects in Metals, Transactions of the Metallurgical Society AIME*, pp. 77-85, 1980.
- [18] J. Tien, A. Thompson, I. Bernstein and R. Richards, "Hydrogen transport by dislocations," *Metallurgical Transactions*, vol. A. 7, pp. 821-829, 1976.
- [19] R. McLellan, "Thermodynamics of diffusion behavior of interstitial solute atoms in non-perfect solvent crystals," *Acta Metallurgica*, vol. 27, pp. 1655-1663, 1979.
- [20] J. Lufrano and P. Sofronis, "Hydrogen transport and large strain elastoplasticity near a notch in alloy X-750," *Engineering Fracture Mechanics*, vol. 59, no. 6, pp. 827-845, 1998.
- [21] P. Kedzierzawski, "Hydrogen degradation of ferrous alloys," *Noyes Publications*, p. 251, 1985.
- [22] J. Hirth, "Stress corrosion cracking and hydrogen embrittlement of iron base alloys," vol. 5, no. 1, 1977.
- [23] R. Fuentes-Samaniego, R. Gasca-Neri and J. Hirth, "Solute drag on moving edge dislocations," *Phil. Mag. A.*, vol. 49, pp. 31-43, 1984.
- [24] D. Symons, "A comparison of internal hydrogen embrittlement and hydrogen environment embrittlement of X-750," *Engineering Fracture Mechanics*, vol. 68, pp. 751-771, 2001.
- [25] D. Saymons, "An investigation into the effects of hydrogen on the fracture and deformation behavior of alloy X-750," Carnegie Mellon University, Pittsburgh, PA, 1994.
- [26] W. Bouajila and J. Riccius, "A first step into modeling hydrogen embrittlement with a commercial Finite Element program," in *4th European Conference for Aerospace Sciences (EUCASS)*, Saint Petersburg (Russia), 2011.
- [27] W. Bouajila and J. Riccius, "Modeling of the internal hydrogen embrittlement effects on the fatigue life of a structure using a commercial F.E. program," in *Space Propulsion*, Bordeaux (France), 2012.
- [28] D. Saymons und A. Thompson, „The effect of hydrogen on the fracture of alloy X-750,“ *Metallurgical and Material Transactions*, Nr. 27, pp. 101-110, 1996.
- [29] Special Metals, "INCONEL alloy X-750," 2004. [Online]. Available: <http://www.specialmetals.com/documents/Inconel%20alloy%20X-750.pdf>. [Accessed 31 08 2012].
- [30] R. Staehle, "Stress corrosion cracking (and corrosion fatigue)," *Materials Science and Engineering*, vol. 25, pp. 207-215, 1976.